AD-A062 830 ARMY MATERIALS AND MECHANICS RESEARCH CENTER WATERTO--ETC F/G 11/4
IN-PLANE SHEAR TEST FOR COMPOSITE MATERIALS.(U)
JUL 78 J M SLEPETZ, T F ZAGAESKI, R F NOVELLO

UNCLASSIFIED AMMRC-TR-78-30 NL

OF
AD
A062 830

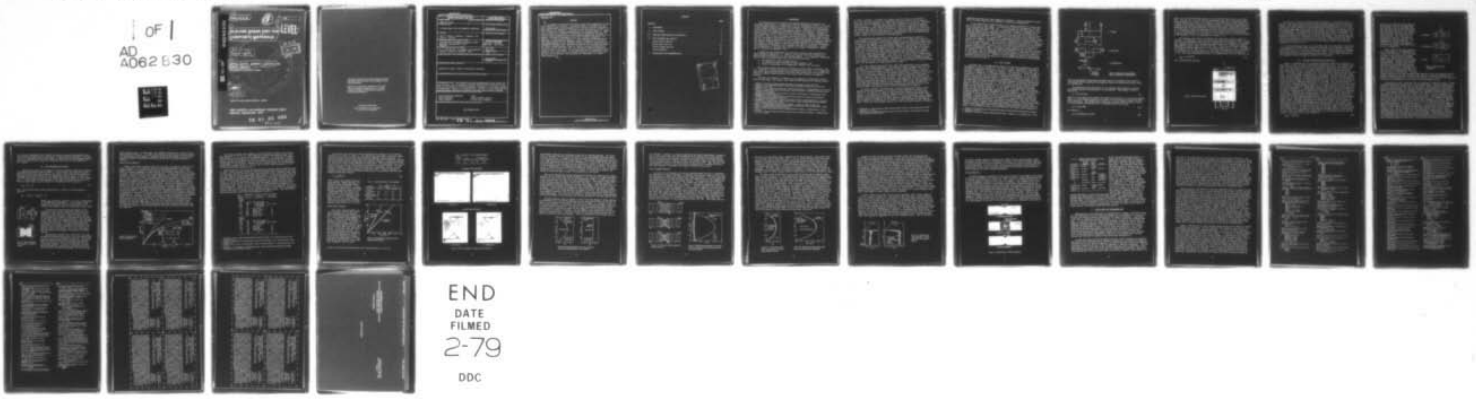

END
DATE
FILMED
2-79
DDC

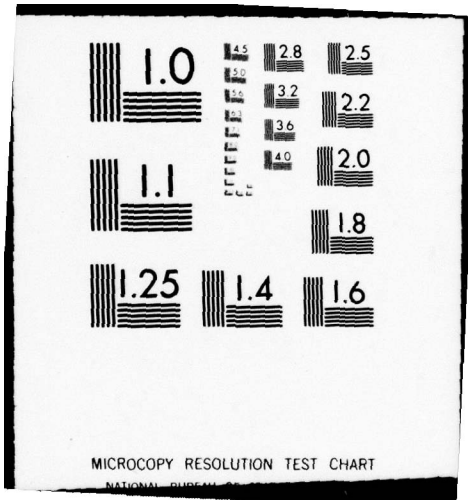
1.0
1.1
1.25
1.4
1.6
1.8
2.0
2.2
2.5
2.8
3.2
3.6
4.0
4.5
5.0
5.6
6.3
MICROCOPY RESOLUTION TEST CHART

(14) AMMRC-TR-78-30

AD

LEVEL II

IN-PLANE SHEAR TEST FOR COMPOSITE MATERIALS.

(9) Final rept.,

(10) JOHN M. SLEPETZ, THEODORE F. ZAGAESKI and ROBERT F. NOVELLO
MECHANICS OF MATERIALS DIVISION

(11) Jul 78
(12) 27 p.

ARMY MATERIALS AND MECHANICS RESEARCH CENTER
Watertown, Massachusetts 02172

The findings in this report are not to be construed as an official Department of the Army position, unless so designated by other authorized documents.

Mention of any trade names or manufacturers in this report shall not be construed as advertising nor as an official indorsement or approval of such products or companies by the United States Government.

DISPOSITION INSTRUCTIONS

Destroy this report when it is no longer needed.
Do not return it to the originator.

UNCLASSIFIED

SECURITY CLASSIFICATION OF THIS PAGE (When Data Entered)

REPORT DOCUMENTATION PAGE		READ INSTRUCTIONS BEFORE COMPLETING FORM
1. REPORT NUMBER AMMRC TR 78-30	2. GOVT ACCESSION NO.	3. RECIPIENT'S CATALOG NUMBER
4. TITLE (and Subtitle) IN-PLANE SHEAR TEST FOR COMPOSITE MATERIALS		5. TYPE OF REPORT & PERIOD COVERED Final Report 6. PERFORMING ORG. REPORT NUMBER
7. AUTHOR(s) John M. Slepetz, Theodore F. Zagaeski, and Robert F. Novello		8. CONTRACT OR GRANT NUMBER(s)
9. PERFORMING ORGANIZATION NAME AND ADDRESS Army Materials and Mechanics Research Center Watertown, Massachusetts 02172 DRXMR-TM		10. PROGRAM ELEMENT, PROJECT, TASK AREA & WORK UNIT NUMBERS D/A Project: M726350 AMCMS Code: MTT Project
11. CONTROLLING OFFICE NAME AND ADDRESS U. S. Army Materiel Development and Readiness Command, Alexandria, Virginia 22333		12. REPORT DATE July 1978 13. NUMBER OF PAGES 22
14. MONITORING AGENCY NAME & ADDRESS(if different from Controlling Office)		15. SECURITY CLASS. (of this report) Unclassified 15a. DECLASSIFICATION/DOWNGRADING SCHEDULE

16. DISTRIBUTION STATEMENT (of this Report)

Approved for public release; distribution unlimited.

17. DISTRIBUTION STATEMENT (of the abstract entered in Block 20, if different from Report)

18. SUPPLEMENTARY NOTES This project has been accomplished as part of the U.S. Army Materials Testing Technology Program, which has for its objective the timely establishment of testing techniques, procedures or prototype equipment (in mechanical, chemical, or nondestructive testing) to insure efficient inspection methods for materiel/material procured or maintained by DARCOM.

19. KEY WORDS (Continue on reverse side if necessary and identify by block number)

Fiber-reinforced composites	Loads
Shear properties	Finite element analysis
Shear strength	Stress-strain diagrams

20. ABSTRACT (Continue on reverse side if necessary and identify by block number)

(SEE REVERSE SIDE)

DD FORM 1 JAN 73 1473 EDITION OF 1 NOV 65 IS OBSOLETE

79 01 02 009

UNCLASSIFIED

SECURITY CLASSIFICATION OF THIS PAGE (When Data Entered)

Block No. 20

ABSTRACT

A new method for characterizing the in-plane shear properties of composite materials is discussed. The method employs an asymmetrical four-point bending (AFPB) load arrangement which subjects the test specimen to pure shear at its centerline: the shear stress distribution at this location is uniform or otherwise depending upon the specimen geometry. Demonstration tests were conducted on specimens of aluminum and two types of fiber-reinforced composites of various specimen geometries including rectangular, vee-notched rectangular, and fillet-notched rectangular. In addition, a finite element analysis of these specimen configurations was undertaken to determine the depthwise stress distribution in each case. Strain measurements on test specimens showed a parabolic distribution in rectangular specimens and a uniform distribution in vee-notched specimens. The finite element analysis, however, showed a stress concentration at the notch root in the latter case, and specimens loaded to destruction tended to fail at the notch. It was concluded that with appropriate modification in the test fixture and specimen geometry the AFPB method developed will be an effective test procedure for measurement of in-plane shear properties.

CONTENTS

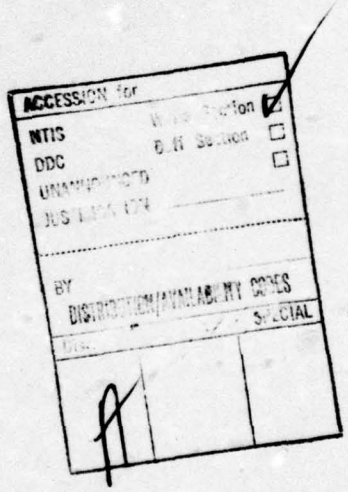

I. BACKGROUND

The characterization of elastic and strength properties of materials for structural applications is accomplished by the use of mechanical tests. As a rule, fiber-reinforced composites require more extensive testing for this purpose than do more common structural materials such as metals. Additional test requirements arise from the anisotropic and heterogeneous nature of composites. Even for the simplest case of a homogeneous anisotropic material, for instance, a minimum of four independent elastic constants must be determined for complete in-plane characterization. This is twice the number required for ideally isotropic material and implies a minimum of three separate tests to determine all four constants, whereas only one is needed to determine the two constants corresponding to material isotropy. The complete characterization of in-plane strength properties of a composite may also require a larger number of tests because the behavior in tension of heterogeneous materials is frequently very different from that in compression. Finally, the determination of in-plane shear modulus and strength of composites, unlike metals, requires an independent test.

A number of test methods have been devised to measure shear properties of fiber-reinforced composites.[1-12] However, in practice these have usually not proved entirely satisfactory for the intended purpose. It is generally recognized that an ideal test method should have the following qualities:

a. be mechanically simple in application,
b. use relatively small specimens of simple geometry, and
c. subject the specimen to an unambiguous, uniform state of stress.

One or more of these qualities is lacking in current shear test methods, and it is difficult to devise a method which incorporates all three. It is largely for this reason that characterization of in-plane shear behavior has been a persistent barrier to complete understanding of the stress-strain response of composite materials.

The shear test methods in frequent use for composites include tube torsion, picture-frame shear, rail shear, cross-sandwich-beam bending, and uniaxial tension

1. CARD, M. F. *Experiments to Determine Elastic Moduli for Filament Wound Cylinders.* NASA TN D-3110, 1965.
2. FELDMAN, A., et al. *Experimental Determination of Stiffness Properties of Thin-Shell Composite Structures.* Experimental Mechanics, v. 8, 1966, p. 385.
3. WHITNEY, J. M., et al. *Analysis of the Rail Shear Test – Applications and Limitations.* J. Composite Materials, no. 5, 1971, p. 24-34.
4. BRYAN, E. L. *Photoelastic Investigation of Stress Distribution in the Panel-Shear Specimen.* Symposium for Shear Torsion Testing, ASTM, STP 289, 1961, p. 90-94.
5. HADCOCK, R. N., and WHITESIDE, J. B. *Characterization of Anisotropic Composite Materials.* Composite Materials: Testing and Design, ASTM, STP 460, 1969, p. 37-47.
6. HENNESSEY, J. M., et al. *Experimental Methods for Determining Shear Modulus of Fiber Reinforced Composite Materials.* Air Force Materials Laboratory, AFML TR 65-42, 1965.
7. BALABAN, M. M., and JACKSON, W. T. *A Method of Testing Thin Webs in Shear.* Experimental Mechanics, v. 5, 1971, p. 224.
8. WADDOUPS, M. E. *Characterization and Design of Composite Materials.* Composite Materials Workshop, Technomic Publishing Co., Inc., Stamford, Connecticut, 1968, p. 254-308.
9. LENOE, E. M. *Testing and Design of Advanced Composite Materials.* J. Eng. Mech. Div. ASCE, v. 96 (EM6), 1970.
10. PETIT, P. H. *A Simplified Method of Determining Inplane Shear Stress-Strain Response of Unidirectional Composites.* Composite Materials: Testing and Design, ASTM, STP 460, 1969, p. 83-93.
11. SIMS, D. F. *In-Plane Shear Stress-Strain Response of Unidirectional Composite Materials.* J. Composite Materials, no. 7, 1973, p. 124-128.
12. HAHN, H. T. *A Note on Determination of the Shear Stress-Strain Response of Unidirectional Composites.* J. Composite Materials, no. 7, 1973, p. 383-386.

of $[\pm 45^\circ]_s$ laminates. In addition to these, there are other test methods[13,14] which have had less general use. Undoubtedly the most suitable of the commonly used tests from the standpoint of stress field uniformity is torsion of a thin-wall composite tube.[1-3] There are some undesirable features of this method, however. One disadvantage is that tubular specimens are relatively expensive to fabricate and require more material than flat specimens. There are complexities in the test application which must be considered also. Difficulties arise in applying the torsional loading to the specimens without introducing axial forces and edge-bending moments along with their associated coupling effects.

Test methods which employ flat rather than curved specimens include the picture-frame shear test[4,5] and the rail shear test.[3,6,7] These tests are relatively simple in application and specimen geometry, but they induce a complex state of stress in the specimen. In the picture-frame shear test the induced stress field is generally nonuniform, which considerably reduces the usefulness of the test in determining stress-strain response in shear. However, near the edges of the specimen it has been reported[4] that the stress state is very nearly that of uniform, pure shear, so that valid shear strength determinations presumably can be made. In the rail shear test the specimen is attached to the test fixture by means of a row of bolts along opposite edges. This gives rise to severe stress concentrations at the edges, particularly when the major Poisson's ratio of the composite is large, as in the case of a $[\pm 45^\circ]_s$ laminate. Consequently, the shear strength determinations obtained in such cases would be invalid. On the other hand, it has been found that valid measurements of shear modulus can be made.[3]

The cross-sandwich beam test[8-10] has been used extensively in the aerospace industry. The specimen employed in this method is made by bonding thin sheets of the composite to a suitable core material to form a sandwich panel. This is cut into a cruciform and tested by subjecting the cruciform to anticlastic bending. The test is relatively simple and the induced stress field is uniform in the central region of the cruciform; however, specimen preparation requires a considerable amount of material, much of which is wasted. Also, the pure shear region is oriented at $\pm 45^\circ$ to the axes of the cruciform. This means that in order to measure the shear properties with respect to the material symmetry axes, the principal axes of the face sheet material must also be oriented at $\pm 45^\circ$ to the cruciform axes. Such a geometry introduces in-plane shear coupling and edge effects which could seriously affect the validity of test results obtained by this method.

An indirect method of measuring the in-plane unidirectional stress-strain response using flat specimens is to subject a [±45] laminate to uniaxial tension.[11,12] If there is no linear or nonlinear shear coupling, the extensional response of the laminate is found to depend directly on the unidirectional shear modulus with respect to the principal axes.[12] It is not necessarily true, however, that the tension strength of the [±45] laminate corresponds to the unidirectional shear strength of a composite as the former is usually governed by free edge effects. Thus, the [±45] laminate tension test does not provide complete information

13. GRESZCZUK, L. B. *Testing Techniques for Filament Reinforced Plastics Symposium.* Air Force Materials Laboratory, AFML TR 66-274, 1967, p. 95-125.
14. GRESZCZUK, L. B. *Shear Modulus Determination of Isotropic and Composite Materials.* Composite Materials: Testing and Design, ASTM, STP 460, 1969, p. 140-150.

regarding unidirectional shear properties; moreover, it does not address the problem of a direct shear test for laminates of arbitrary configuration.

A test method which eliminates many of the adverse qualities of current methods is described in this report. This method is hereafter designated as the asymmetrical four-point-bend (AFPB) test. It is performed on relatively small, flat, simple geometry specimens. The test is mechanically simple to implement and subjects the specimen to an unambiguous stress field. The stress distribution is determined from elementary beam bending theory provided that the in-plane tension and compression properties of the composite in the direction of the specimen axis are linearly elastic. The present test configuration evolved from an earlier method in which two composite specimens were sheared simultaneously as fixed-end beams.[15] Before this, however, a test device similar in principle was developed by Iosipescu[16] for use on metal specimens. This earlier test method was apparently never standardized or applied to other materials, but later discussion here will show that the specimen configurations used in Iosipescu's study, together with the AFPB test device developed here, offer a very promising technique for shear testing of composite materials. The test apparatus used in the AFPB test is described in Section II of this report while the development of specimen geometry for use with composites is discussed in Section III. Results of a test program on composite and aluminum specimens together with the results of a finite element analysis of specimen geometry are given in Section IV.

II. TEST FIXTURE

The shear test is accomplished by means of a four-point asymmetrical loading arrangement as shown in Figure 1a. The interior loads, separated by a distance b, are equal in magnitude but opposite in sense. Likewise, the exterior loads, separated by a distance a, are equal and opposite. The specimen is loaded on edge, in the plane of lamination, to determine in-plane shear properties. It is worthwhile noting that it would also be possible to measure shear properties in the thickness plane by loading the specimen normal to the plane of lamination; however, the discussion which follows will be limited to determination of in-plane properties only. The shear force and bending moment distribution produced by the given load arrangement are shown in Figures 1b and 1c. The shear force is constant and the bending moment is decreasing in absolute value in the region between the interior load points and the specimen centerline. At the center of the specimen the bending moment is zero, and the specimen is in pure shear. The shear stress distribution across the depth of the specimen depends on its configuration. For a uniform depth, constant thickness specimen, elementary beam theory predicts a parabolic stress distribution, which varies from zero at the top and bottom edges to a maximum at mid-depth. This distribution is based on equilibrium considerations, linear distribution of normal strains across the depth (i.e., plane sections remain plane), and linear stress-strain behavior in tension and compression. Note that, theoretically at least, the shear stress distribution does not require linear stress-strain behavior in shear. However, nonlinear shear behavior resulting in large shear strains would undoubtedly affect the assumption regarding plane sections remaining plane. In the absence of gross nonlinear behavior, the stress-strain response in

15. SLEPETZ, J. M. *Elastic Characterization of Fiber Reinforced Composites.* Composite Materials, AGARD Conference Proceedings, no. 63, 1971, p. 8-1 to 8-8.
16. IOSIPESCU, N. *New Accurate Procedure for Single Shear Testing of Metals.* J. Materials, v. 2, no. 3, September 1967, p. 537-566.

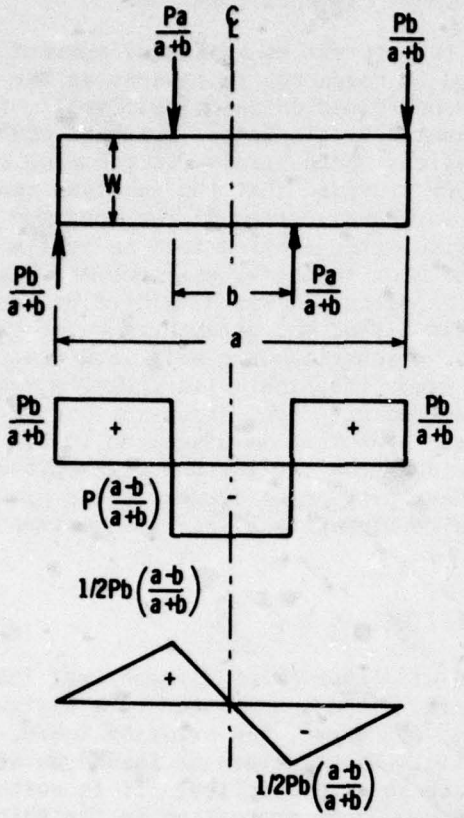

a. Loading

b. Shear Force

c. Bending Moment

Figure 1. Load, shear force, and bending moment relationships for AFPB specimens.

shear is determined by measuring the shear strain at mid-depth of the center of the specimen and by employing the elementary theory to calculate the shear stress at a given load.

The magnitude of the shear force in the constant shear region is governed by external equilibrium requirements of the specimen. From Figure 1b this is seen to be

$$V_1 = P(a-b)/(a+b) \tag{1}$$

where V_1 is the shear force between the interior load points, P is the total applied force, a is the distance between the exterior, and b the distance between the interior load points. The maximum shear stress for a uniform depth specimen is given by the well-known relationship for a rectangular beam cross section

$$\tau_m = 3/2(V_1/Wh) \tag{2a}$$

or, from Eq. 1

$$\tau_m = 3/2(P/Wh)(a-b)/(a+b) \tag{2b}$$

where τ_m is the maximum shear stress, W is the specimen depth, and h is the thickness. From Eq. 2b it is seen that the magnitude of τ_{max} can be adjusted by manipulating dimensions a and b. For purposes of load efficiency it might appear that b should be very small; however, in order to maintain a reasonably large region of constant shear force and negligible bending stresses (since strain gages of finite dimensions must be used in practice), and avoid edge-loading effects in this region, it is advisable to keep this dimension at least as large as the specimen depth W. As it is also desirable to insure failure in the central region of the specimen, it may be necessary that $V_1 > V_2$ where V_2 is the shear force in the exterior regions of the specimen. This is accomplished by setting $a > 2b$.

The prototype test fixture for applying the four-point loading is shown in Figure 2. The apparatus, shown here with a glass/epoxy specimen installed, is used in a tension test machine with universal linkages for load alignment. This arrangement eliminates many of the alignment problems inherent in a compression loading mode commonly used in other types of bend tests. The fixture in Figure 2 permits variation of specimen depth up to 1.75 in. and thickness up to 1.2 in. The distance a is fixed at 5.5 in. and b at 2.5 in. The choice of dimensions a and b was made in accordance with the requirements just discussed and satisfies the condition $a > 2b$. This load configuration results in a maximum shear stress of (from Eq. 2b)

$$\tau_{max} = 9/16(P/Wh) \qquad (3a)$$

for a uniform depth specimen.

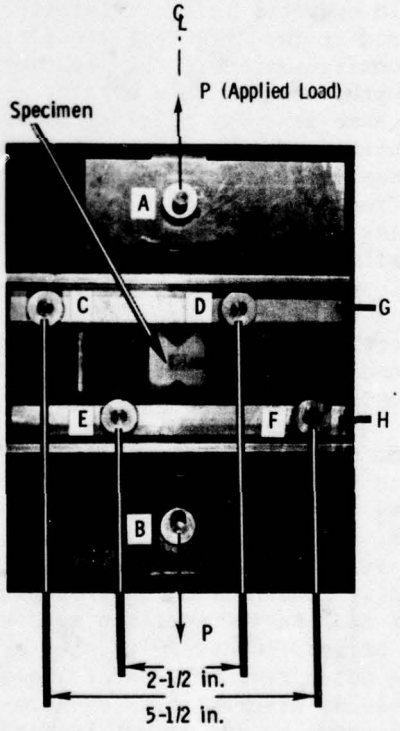

Figure 2. AFPB test fixture details.

The details of the test fixture are seen in Figure 2. The central load P is applied to the top and bottom of the fixture through hardened steel pins at points A and B. The load on each side of the fixture is then distributed to the top and bottom edges of the specimen as concentrated forces through pins at C, D, E, and F. The relative magnitude of the force at these points is fixed by the geometry of the load arrangement. The displacement of the specimen and fixture is constrained to a vertical plane by the angles G and H attached to both sides of the fixture. The maximum load rating for the present fixture is 5000 pounds. This capacity and the dimensional flexibility with respect to W and h are adequate for most characterization test requirements involving composite materials. Demonstration tests were carried out as described in Section IV with satisfactory results using specimen dimensions of 1.5 in. × 6 in.

To avoid crushing the edges of the specimen under the concentrated load points, it was necessary to attach steel doublers to both ends of the specimen. The full width doublers, 2.0 in. long, were adhesively bonded to both sides of the specimen, leaving the central 2.0-in. region of interest clear. This arrangement was found to be satisfactory for avoiding possible complications in the stress field due to load transfer in shear through the doublers to the specimen.

III. SPECIMEN CONFIGURATION AND MATERIALS

Ideally, any mechanical test specimen configuration should be as simple as is practicable in order to reduce machining and preparation costs. The composite specimens required in the AFPB test are flat laminates with overall rectangular geometry. This configuration is the least expensive to manufacture and, in the case of uniform depth, results in a parabolic theoretical shear stress distribution which is the same at every interior cross section at points removed from the applied loads. The uniform depth configuration is satisfactory for measuring shear stress-strain response; however, it would be more advantageous to have a specimen configuration which resulted in a uniform stress distribution. Moreover, for purposes of measuring shear strength, it would be desirable to have only one section, preferably at the centerline, where the shear stress is a maximum. This would preclude the likelihood of specimen failure occurring in the vicinity of one of the interior load points under a state of combined stress, as is the most probable event in the case of uniform depth geometry. Preferably, failure should occur at the centerline under pure shear conditions. A varying depth configuration would obviously be required to obtain a uniform depthwise shear stress distribution, if indeed such a condition is possible. Moreover, the minimum section would have to be at the centerline to obtain maximum shear stress at that location. Such a condition was achieved by Iosipescu[16] in metal specimens machined with 90° vee-notches at the top and bottom edges, leaving a net section depth at the specimen centerline of one half of the overall depth. Iosipescu confirmed the uniform state of pure shear by means of photoelastic strain field measurements on plexiglass models. The uniform stress state apparently results from the fortuitous coincidence of the principal stress directions at ±45° to the specimen axis with the 90° notch angle in the region of zero bending stress. Contrary to what might be expected, there is no stress singularity at the notch root because of the absence of normal stresses at this point. If shear stress is assumed to be uniform across the vee-notched section, then the stress is not given by Eq. 3a but instead by

$$\tau_{max} = 3/8(P/Wh) \qquad (3b)$$

where W is now the net section depth of the specimen. Unlike the simple beam result given by Eq. 3a, the above equation may not be theoretically valid for nonlinear shear behavior or for complexities arising at the notch root due to shear coupling. This aspect will be discussed in Section V. Iosipescu's investigation was concerned only with homogeneous, isotropic materials. It remained to be shown in the present study that the results have application as well to composites.

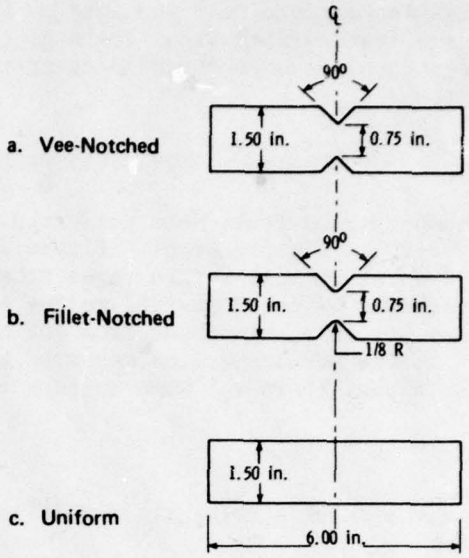

Figure 3. AFPB test specimen configurations.

Three different specimen geometries were investigated in the demonstration study of the AFPB test. These are shown in Figure 3 and include the Iosipescu specimen, a variation having rounded rather than sharp notches, and a uniform depth specimen. Several other specimen configurations, including semicircular edge-notched and slotted edge-notched, were also considered for investigation but were rejected after preliminary tests showed that the induced stress field in each case was not satisfactory. A finite element analysis of the three specimen types employed in the investigation was conducted to determine the stress field in each case as a function of geometry and material elastic properties. The details and results of this analysis are discussed along with the demonstration test results in the following section.

The materials used to fabricate the test specimens included two types of fiber-reinforced composites and one metal, 2024 aluminum alloy. The 2024 aluminum alloy served as the control material as its shear stress-strain properties have already been well characterized. The composite materials investigated were glass/epoxy (marketed by the 3M Company as Scotchply 1002S) and graphite/epoxy (Narmco Modulite II). Two different laminate configurations were employed for each composite, unidirectional and $[0,90]_s$ cross ply. Panels, 24 × 24 in., of each composite were fabricated by a tape lay-up and autoclave cure process. Glass/epoxy panels were 12 plies thick having a nominal total thickness of 0.11 in., whereas the graphite panels were 8 plies thick and had a nominal total thickness of 0.08 in. The nominal volume fraction of fibers was 55% in the case of glass/epoxy and 60% for graphite/epoxy panels. Rectangular blanks 1.5 × 6 in. were cut from the composite panels and machined to the prescribed geometry. Four specimens of each composite material, each laminate sequence, and each notch geometry were used in the demonstration tests. The one exception to this test plan was that fillet-notched specimens were used only in the case of unidirectional graphite/epoxy. Uniform depth specimens only were used in the case of aluminum. Unidirectional specimens were machined with the reinforcement direction parallel to the longitudinal axis of the specimen, and cross-ply specimens were made with the outer ply reinforcement direction parallel to that axis. This was done arbitrarily in the case of

the cross-ply specimens, but it served the purpose of preventing unwanted transverse tension failure near the load points in unidirectional specimens. The specimens were instrumented with strain gages or other strain field measurement device, and steel doublers were attached as previously described in final preparation for testing.

IV. TEST PROCEDURE AND RESULTS

Demonstration tests were performed on metal and composite specimens using the prototype shear fixture seen in Figure 2. In most cases, specimens were instrumented with electrical strain gages at mid-depth on both sides of the centerline. The gages were oriented at ±45° to the longitudinal axis as shown in Figure 4a. The shear strain γ_{xy} is found from the normal strain measurements at these orientations. If the normal strains measured by the gages are designated as ε_x' and ε_y', then the shear strain γ_{xy} with respect to the specimen axis is given by

$$\gamma_{xy} = \varepsilon_x' - \varepsilon_y'. \tag{4}$$

Also, if the shear stress-strain relationship is linear, the shear modulus is given by

$$G_{xy} = \tau_{xy}/\gamma_{xy} = \tau_{max}/\varepsilon_x' - \varepsilon_y' \tag{5}$$

where τ_{max} is given by either Eq. 3a or Eq. 3b according to the specimen configuration. If the stress-strain response is nonlinear, then the shear modulus is the slope of the response curve at a particular strain level.

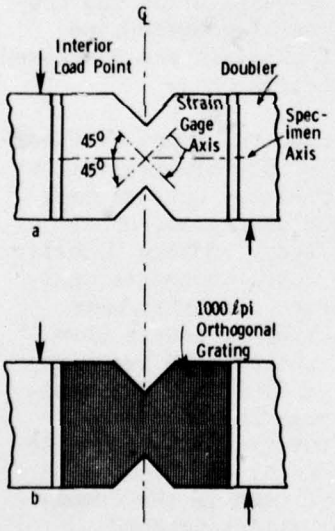

Figure 4. Strain measurement instrumentation for AFPB test specimen.

In addition to strain gage measurements at the centerline, moiré fringe interference techniques were employed in some cases to provide full-field strain analysis of test specimens. Figure 4b shows a sketch of a specimen with a moiré grating mounted on one side in the area between the loading doublers. The gratings used in this study had orthogonal rulings with a density of 1000 lines per inch. This permitted simultaneous measurement of orthogonal specimen displacements from which the shear strains everywhere in the field of the grating could be determined. Electrical strain gages were provided on the specimen side opposite the moiré grating.

Instrumented specimens were installed in the AFPB fixture and loaded quasistatically at a cross-head speed of 0.02 in./min in an Instron test machine. The strain gage and load transducer output signals were recorded on an X-Y plotter to obtain a continuous history of load-strain response. In tests on specimens provided with moiré gratings, loading was interrupted at convenient intervals to permit photographs to be made of the

moiré fringe pattern. In some cases, the procedure followed was to load the specimen directly to failure. In others, the load was cycled several times to observe the load-unload strain response. Specimens which had been loaded to failure were examined visually to determine the location of failure initiation and mode of failure.

Stress-Strain Behavior

Typical load-strain response curves for two types of composite specimens are shown in Figure 5. The curves are for 90° vee-notched specimens of cross-ply graphite/epoxy in one case and unidirectional glass/epoxy in the other. Since stress is linearly dependent on load, from Eq. 3b the load-strain history is also, in effect, the stress-strain curve of the material. In each case the stress-strain response in Figure 5 is seen to be highly nonlinear above strains of the order of 0.01 in./in. In view of this, the shear modulus must be defined as either the tangent or secant modulus at a specified strain level in order to have a consistent meaning as a material property. In the experiments here the modulus was taken as the initial slope G_t of the stress-strain curve. The initial tangent modulus was found to be 0.90×10^6 psi for the unidirectional glass/epoxy specimens and 0.86×10^6 psi for the cross-ply graphite/epoxy specimens. The mean values of G_t obtained for the four laminate types and three specimen configurations employed in the study are given in Table 1. In general, there was no significant difference in values of G_t obtained for specimens of the same composite type but having different geometric configurations. In fact, the range of values for a particular geometry was somewhat larger than the difference in mean values among the various geometries tested. There was also very little difference in G_t between cross-ply and unidirectional specimens for the two composites. This was to be expected, as laminate theory predicts the in-plane shear modulus of a $[0,90]_s$ lay-up to be the same as for a unidirectional lay-up. The small differences that were observed are probably due to slight variations in fiber volume fraction between the unidirectional and cross-ply laminates.

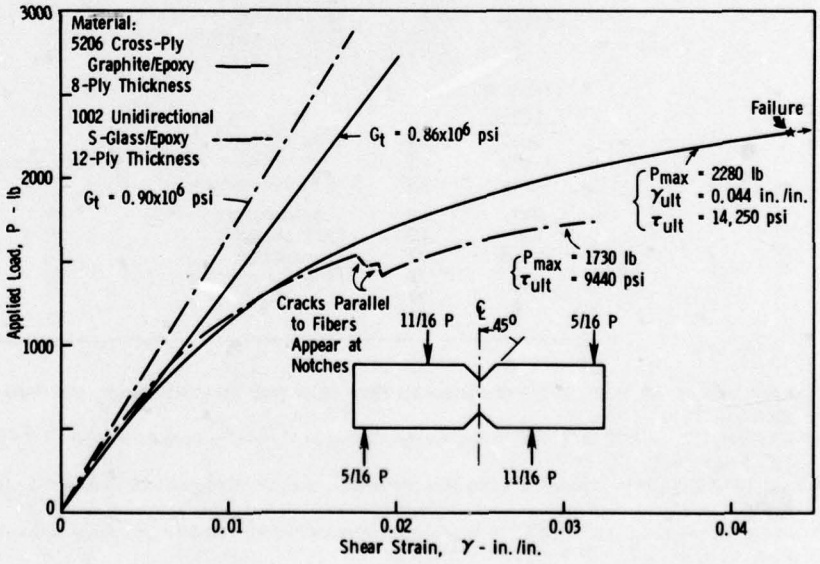

Figure 5. Load-strain history of composite specimens.

Also shown in Table 1 are average G_t values obtained elsewhere using various test methods.[2,10,11,13,14,17] Some differences between the reported values and those obtained by the AFPB test are apparent; however, it is difficult to compare results from one investigation to another because it is seldom possible to match material processing variables such as fiber volume fraction in the test materials. In Reference 14, for instance, reported values of shear modulus for unidirectional S-glass/epoxy ranged from 0.61×10^6 psi for 51% fiber volume fraction to 1.34×10^6 psi for 69% fiber volume fraction.

The similarity of G_t values for glass/epoxy and graphite/epoxy composites seen in Table 1 occurs because the matrix material properties were essentially the same in both cases, and the two fiber types, despite having widely different Young's moduli, have nearly the same longitudinal shear modulus. It has been shown[18] that the in-plane composite shear modulus depends primarily on the fiber shear modulus and the properties of the matrix material rather than on the Young's modulus of the fiber. To illustrate this point Table 2 summarizes the average in-plane elastic properties of the unidirectional glass/epoxy and graphite/epoxy specimens used in the present study, as well as the individual constituent material properties of these composites. Young's modulus and Poisson's ratio of the composites were determined by tension tests on 3/4 × 9 in. coupons, and the G_t values are the average of all the AFPB tests, including notched and uniform depth results. The constitutive material properties were taken from References 19 and 20.

Table 1. COMPARISON OF G_t VALUES BY VARIOUS TEST METHODS

Material	G_t, psi	Test Method	Reference
S-Glass/ Epoxy			
Uni.	0.87×10^6	AFPB Uniform depth	This study
Uni.	.89	Vee-notched	
X-ply	.85	Uniform depth	
X-ply	.83	Vee-notched	
Uni.	1.44	Tube torsion	2
↓	1.27	Off axis tension	13
↓	0.61	Douglas ring	14
X-ply	0.80	Rail shear	11
↓	0.78	$[\pm 45°]_s$ tension	11
↓	0.75	Douglas ring	14
Graphite/ Epoxy			
Uni.	0.84	AFPB Fillet notched	This study
X-ply	.88	Uniform depth	
X-ply	.89	Vee-notched	
Uni.	.69	Tube torsion	11
Uni.	.83	Rail shear	17
X-ply	.77	Cross-beam	10
↓	.75	$[\pm 45°]_s$ tension	10
↓	.97	↓	11
↓	.81	↓	11

17. LACKMAN, L. M., et al. *Advanced Composites Data for Aircraft Structural Design.* Air Force Materials Laboratory, AFML TR 70-58, 1972, p. 82.
18. HALPIN, J. C., and TSAI, S. W. *Environmental Factors in Composite Materials Design.* Air Force Materials Laboratory, AFML TR 67-423, 1967.
19. ASHTON, J. E., et al. *Primer on Composite Materials: Analysis.* Technomic Publishing Co., Inc., Stamford, Connecticut, 1969, p. 113.
20. BROUTMAN, L. J., and KROCK, R. H. *Fiber-Reinforced Plastics.* Modern Composite Materials, Addison-Wesley, Reading, Massachusetts, 1967, p. 307-309 and p. 338-343.

Load-strain test results for 2024 aluminum alloy specimens of two different thicknesses are given in Figure 6. The load-unload cycle shows essentially linear behavior in both cases but with some hysteresis apparent during unloading. The latter phenomenon is most likely due to friction at some point between the specimen and load fixture because aluminum does not ordinarily exhibit a measurable hysteresis loop at the strain levels employed in these tests. The implications of friction forces active in the test device will be discussed in the next section. The same aluminum specimens tested in the AFPB fixture were subsequently tested in axial tension to determine Young's modulus and Poisson's ratio. Because aluminum is isotropic, the well-known relationship between those two properties and the shear modulus should apply; namely,

$$G = \frac{E}{2(1 + \nu)}. \tag{6}$$

Table 3 gives the average values of shear modulus, Young's modulus, and Poisson's ratio determined experimentally for each specimen. A comparison can be made of G_c, calculated from Eq. 6 using the values of E and ν determined from the tension test, and the value of G measured in the AFPB test. In both instances these agree to within 1%. The measured value of G is also within a few percent of the accepted value for 2024 aluminum alloy, which is 4×10^6 psi.

Table 2. ELASTIC PROPERTIES OF TEST MATERIALS

Material	E_x (psi)	E_y (psi)	G_t (psi)	ν
Uni. S-glass/ epoxy	6.2×10^6	1.75×10^6	0.88×10^6	0.29
Uni. graphite/ epoxy	19.8	1.21	0.84	.28
S-glass fibers	12.4	12.4	5.0	.22
Mod II graphite fibers	35	-	4.0	.21
Epoxy resin	0.5	0.5	0.19	.35

Moiré Strain Analysis

The strain field uniformity of vee-notched and uniform depth glass/epoxy specimens was investigated using moiré interference fringe analysis. The sequence of photographs in Figure 7 shows the fringe patterns obtained in each case. In Figures 7a and 7b the moiré fringe pattern at zero and 800-lb applied load are shown for the uniform depth specimen; and in Figures 7c and 7d at zero and 500-lb for the vee-notched specimen. The moiré fringe pattern is an analog of the specimen displacement field[21] in which the two families of fringes, developed by interference of a fixed grating and one attached to the specimen, represent lines of equal

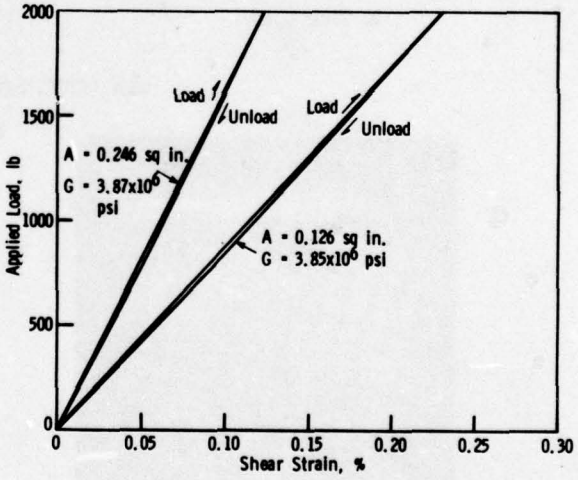

Figure 6. Load-displacement response of uniform depth aluminum specimens.

21. POST, D. *The Moiré Grid-Analyzer Method for Strain Analysis.* Experimental Mechanics, no. 5, 1965, p. 368.

Table 3. PROPERTIES OF 2024 ALUMINUM SPECIMENS

Thickness (in.)	E (psi)	ν	G (psi)	G_c (psi)
0.10	10.3×10^6	0.33	3.85×10^6	3.88×10^6
0.16	10.2	0.31	3.87	3.90

UNIFORM DEPTH SPECIMEN

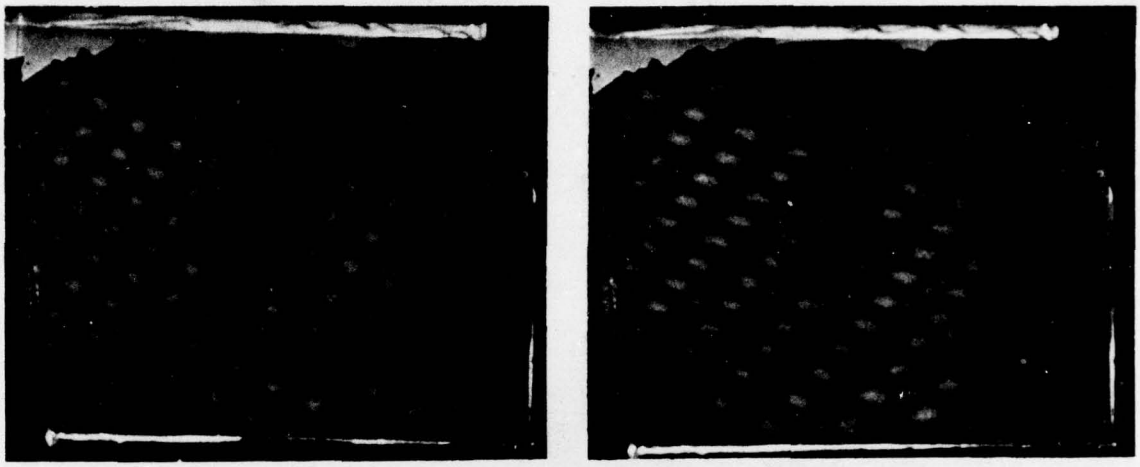

a. Zero Load

b. 800-lb Load

VEE-NOTCHED SPECIMEN

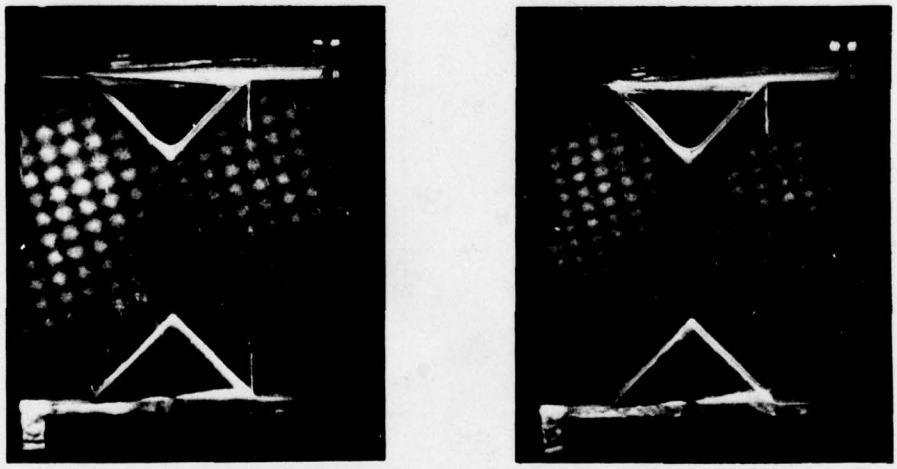

a. Zero Load

b. 500-lb Load

Figure 7. Moiré fringe patterns of S-glass/epoxy shear specimens.

displacement along the two orthogonal directions of specimen grating. The strain field is obtained from the first derivatives of the displacement functions along the same directions. Procedures have been developed for determining these derivatives numerically from a given fringe pattern. The primary displacements associated with shear deformation are rotations; consequently, in these tests an initial rotational mismatch of the specimen grating was applied in order to improve the accuracy of strain measurement by increasing the number of fringes in the field. The shear strain is deduced from the difference between the moiré pattern at a given load and the pattern at zero load. It is given, in effect, at a particular point by the change in fringe spacing and angle of orientation at that point.

The strain distribution can be observed qualitatively by comparing the fringe patterns for the loaded and unloaded conditions. For instance, in comparing Figures 7a and 7b it can be seen that one set of displacement fringes in Figure 7b became closer together while the other set moved further apart. The largest change appears to have occurred near mid-depth of the field, and there is a gradual decrease in fringe spacing difference toward the top and bottom edges. This indicates that the strain-field has a depthwise gradient and that the maximum strain occurs at about mid-depth. Figure 8a shows the depthwise strain distribution obtained by a quantitative analysis of the fringe patterns of Figures 7a and 7b. The observed distribution compares reasonably well with the parabolic strain distribution predicted by simple beam theory. Also shown in the figure is the mid-depth shear strain measured by electrical gages on that specimen and similar specimens at the same applied load.

The moiré patterns seen in Figures 7c and 7d show the change in fringe spacing and orientation of a vee-notched specimen in the load interval from zero to 500 lb. Along a line connecting the notches, the pattern of change, in contrast to that of the uniform specimen, is essentially the same across the specimen depth, indicating a uniform strain distribution. The actual strain distribution obtained by moiré fringe analysis is plotted in Figure 8b and compared to the theoretical uniform distribution according to Iosipescu. The mid-depth strains measured by electrical gages are also given here. The moiré results for the vee-notched specimen show a generally uniform strain distribution. Strain concentration at the notch roots is

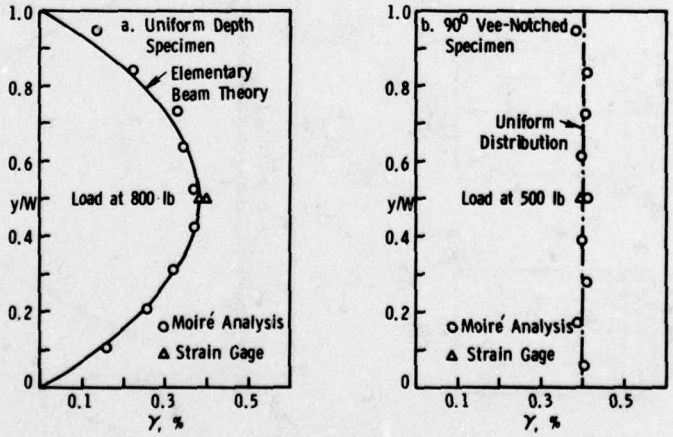

Figure 8. Moiré fringe depthwise shear strain variation in unidirectional 1002 S-glass/epoxy shear specimens.

not indicated. However, it should be mentioned that moiré measurements in general tend to lose sensitivity near the boundaries of the grating due to edge effects. Had a finer density than the 1000 lpi grating been employed, and fringe multiplication techniques used to improve accuracy, the analysis might well have detected a strain concentration in the near vicinity of the notch root. Away from the specimen boundaries, however, the moiré results obtained can be considered reliable, and these indicate a reasonably wide region of uniform shear strain.

Finite Element Analysis

To assist in the evaluation of various specimen geometries and to complement the experimental studies undertaken, a computer-aided elastic analysis of the shear test specimen was carried out using finite element techniques. The same three specimen geometries and the same materials that were employed in the test program were also investigated in the finite element analysis. The composites were modelled as homogeneous, orthotropic materials. The element mesh arrays used for the three specimen configurations are shown in Figure 9. The material properties employed in the analysis were taken from Tables 2 and 3. Because symmetry could not be exploited due to the load arrangement, it was necessary to model the entire specimen in the analysis. While this imposed some limitations in the fineness of the element mesh array which could be used, the accuracy of the analysis was adequate in most cases for computing shear stress distributions in the various specimen configurations. Figure 10 shows the depthwise distribution of in-plane centerline normal and shear stresses of a uniform depth aluminum specimen. These have been normalized with respect to the average shear stress (Eq. 3b). The normal stresses

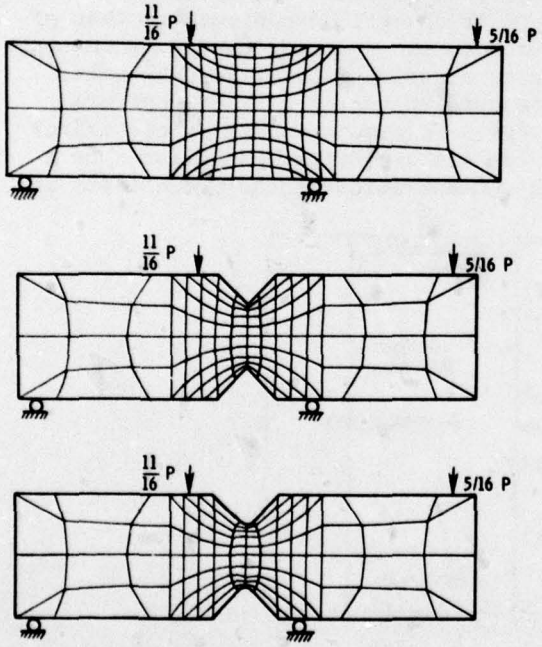

Figure 9. Finite element meshes employed for AFPB test specimen.

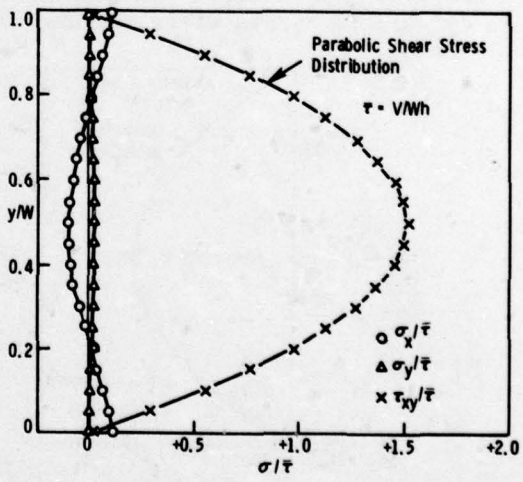

Figure 10. Depthwise stress distribution at centerline of uniform depth aluminum AFPB test specimen by finite element analysis.

are seen to be negligibly small, compared to the shear stresses. The axial stress $\sigma_x/\bar{\tau}$ is about 4.3% of the shear stress. This is consistent with axial strain measurements on aluminum shear specimens and indicates that normal stresses in the region of interest should not have a significant effect on either stress-strain response or failure behavior. Computed normal stresses were higher in the case of aluminum specimens than in the case of either glass/epoxy or graphite/epoxy specimens. The shear stress distribution in Figure 10 is seen to be in excellent agreement with the parabolic distribution predicted by elementary beam theory, the maximum stress by finite element analysis being within 1.5% of the theoretical value.

The shear stress distribution in two types of uniform depth composite specimens is shown in Figure 11a. The magnitude of normal stresses was insignificantly small for both materials. Note that the stress distribution deviates somewhat from parabolic, especially near mid-depth where the shape is flatter and the maximum value differs from the theoretical value by 4.7% for unidirectional glass/epoxy and 10.4% for cross-ply graphite/epoxy. This indicates that a significant error could result in determining shear properties if a parabolic stress distribution were to be assumed for uniform depth composite specimens. The results also indicate that the actual stress distribution depends on material properties, in contradiction to the simple beam theory. If differences in linear elastic properties are important, then nonlinear shear properties of real composites can be expected to have a significant effect on stress distribution. The finite element results for a glass/epoxy specimen are compared to the moiré strain field measurements in Figure 11b. To make the comparison, the stresses determined analytically were converted to strains using a secant modulus of $G_s = 0.72 \times 10^6$ psi, which was consistent with the measured value at the applied load during the test. This is a reasonable procedure for comparison purposes as the shear strains are nearly linear at this load level. The agreement between analytical and measured values is seen to be reasonably good over the specimen depth; in fact, better than the agreement between the latter and parabolic strain distribution mentioned previously.

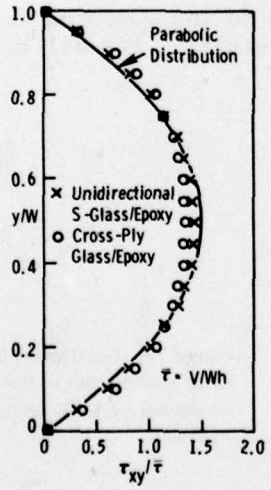

Figure 11a. Finite element analysis shear stress distribution for uniform depth composite specimens.

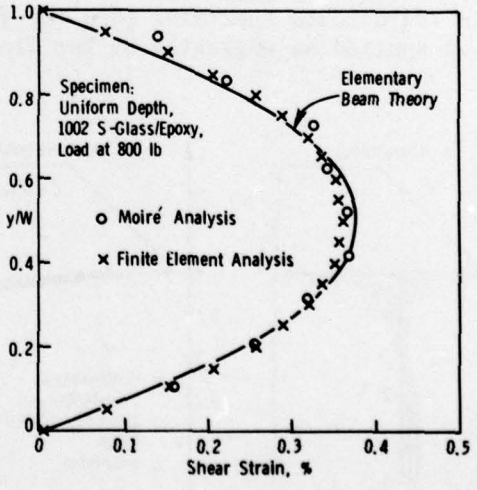

Figure 11b. Comparison of finite element results with moiré fringe shear strain distribution.

Figures 12a and 12b show the finite element results for vee-notched and fillet-notched specimen configurations. In the case of the vee-notched the computed stress distribution is relatively uniform for aluminum and cross-ply graphite/epoxy, but it is seen to increase sharply near the notches for unidirectional glass/epoxy. The analysis employed was not appropriate for determining if the stress condition was singular at the notches; however, it did indicate that the stress concentration increased sharply with the degree of material anisotropy. Results for unidirectional graphite/epoxy indicated an even more severe notch stress concentration than for the unidirectional glass/epoxy. It should seem that the concentration in this case arises from shear coupling along the flanks of the 45° vee-notch, which results in strains that cannot be accommodated due to compatibility requirements. The net effect is a redistribution of in-plane stresses along the notch section and the consequent stress concentration at the notch. The shear coupling occurs because the unidirectional laminate is not orthotropic with respect to the normal stresses which must obtain along the notch flanks. The higher the degree of anisotropy, the stronger the effect of shear coupling. In the case of $[0,90]_s$ cross-ply laminates, orthotropy is retained along the notch flank; thus, there should be no shear coupling and no stress concentration. For nearly all other laminate configurations (a notable exception being the $\pi/4$ — quasi-isotropic laminate), some degree of shear coupling can be expected.

Finite element results for fillet-notched specimens, with a notch radius of 0.125 in., appear in Figure 12b. The analysis shows the shear stresses tending toward zero at the notch root, increasing to a maximum at about one-eighth of the depth, and then becoming reasonably uniform in the central region of the specimen. The results are much the same for all three materials involved. The stress in the uniform region exceeds the average shear stress about 10%, more or less independently of the specimen material properties. The maximum stress exceeds the average stress by abcut 20%, depending on the material. No moiré strain measurements were made on this specimen configuration; however, in determining the stress-strain response, results for this specimen geometry were consistent with those of uniform depth and vee-notched specimens when the 10% adjustment to the computed average stress was applied as suggested by the finite element results. For all materials,

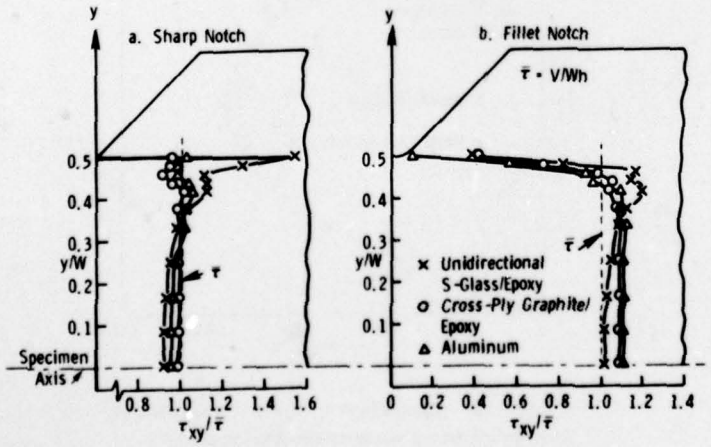

Figure 12. Depthwise shear stress distribution in notched specimens by finite element analysis.

the finite element analysis indicated that normal stresses were negligibly small everywhere at the centerline, including the notches. Any effect of shear coupling on stress distribution at the centerline is alleviated by the zero stress condition at the round notch. In view of this, the fillet notch geometry would appear to be potentially the most useful specimen configuration of the three for both stress-strain response and shear strength measurement.

Failure Behavior

A limited number of specimens of each type of material and geometry were tested to failure to determine the location and mode of failure. Typical specimen failures of various types are shown in Figure 13. This aspect of the demonstration tests was not altogether successful for a number of reasons. The strength of the 12-ply unidirectional and cross-ply S-glass/epoxy uniform depth specimens exceeded the capacity of the test device, so that no failures were obtained for these two cases. The fillet-notched unidirectional graphite/epoxy specimens were machined by mistake with the fiber reinforcement direction perpendicular, rather than parallel, to the specimen axis. This resulted in invalid test results for shear strength as the specimens tended to fail at the loading points in axial tension. This was especially unfortunate since these were the only specimens made with this particular geometry. Figure 13a shows the vee-notched unidirectional S-glass/epoxy specimen for which the load-strain history was given in Figure 5. Shear cracks parallel to the reinforcement can be seen in the moiré grating on the specimen in the vicinity

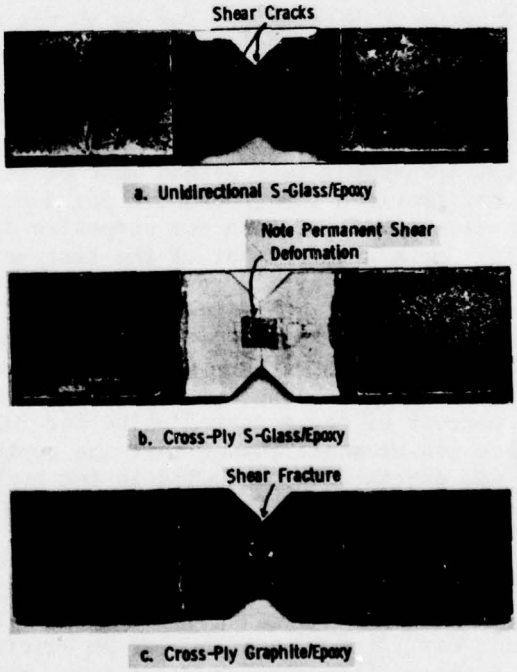

Figure 13. Typical failures in AFPB test-specimens.

Table 4. SUMMARY OF RESULTS ON SHEAR TEST MODE OF FAILURE AND LOCATION

Material	Specimen Geometry	Failure Mode	Location
Uni. S-glass/ epoxy	Uniform	None obtained	-
Uni. S-glass/ epoxy	Vee-notch	Shear	Notch root
X-ply S-glass/ epoxy	Uniform	None obtained	-
X-ply S-glass/ epoxy	Vee-notch	Shear	Mid-depth-centerline
Uni. graphite/ epoxy	Uniform	Shear	Mid-depth-centerline
	Vee-notch	Shear	Notch root
	Fillet notch	Tension	Load point
X-ply graphite/ epoxy	Uniform	Bending/ shear	Doubler
X-ply graphite/ epoxy	Vee-notch	Shear	Notch root

of the top and bottom notch roots. In Figure 13b the vee-notched cross-ply glass/epoxy specimen seen was loaded to the limit of the test fixture without fracturing. The permanent shear strain that was incurred is evident from the distorted appearance of the strain gage at the center of the specimen. The vee-notched cross-ply graphite/epoxy specimen seen in Figure 13c failed in shear; however, the fracture initiated at the notch root. Table 4 summarizes the results of tests conducted to failure. It is important to note that ideal failure conditions (i.e., shear at mid-depth of centerline section) were obtained only in two cases. In view of this and the results obtained in the finite element analysis it appears necessary to conduct additional testing on fillet-notched specimens of various material types and laminate configurations to fully evaluate the effectiveness of the AFPB test method. It appears adequate to use uniform depth specimens for testing unidirectional composites, but not for other laminate types. Vee-notched specimens, on the other hand, appear to be undesirable for shear strength measurement in all cases since failure seems to initiate at the notch root even with laminate configurations for which the moiré results showed a uniform strain distribution across the notch section.

V. CONCLUSIONS AND RECOMMENDATIONS

Demonstration of the AFPB shear test method must be judged a qualified success. The work reported here has provided the groundwork for development of a shear test fixture and suitable specimen configuration for composite materials. Some additional work is needed for further refinement of the test method and specimen geometry. It was shown that the stress-strain response in shear of various types of composite laminates would be reliably obtained short of failure with any of three different specimen geometries. The shear modulus of an aluminum alloy control material was determined to within 1% of the value corresponding to the isotropic relationship between shear modulus, Young's modulus, and Poisson's ratio; this value was within a few percent of the accepted value for 2024 aluminum alloy. Moiré fringe interference measurements showed that the depthwise strain distribution at the centerline was essentially parabolic in the uniform depth specimen geometry and essentially uniform in the vee-notched configuration.

On the other hand, the finite element analysis, while confirming the parabolic and uniform stress distribution in isotropic specimens of the respective geometries, indicated that in the case of composites, the stress distribution deviates somewhat from ideal conditions and may in fact be dependent on material properties. This was particularly true in the case of the Iosipescu specimen where a significant stress concentration was found at the notch root in unidirectional laminates. Shear coupling deformations along the notch flank are believed to impose a redistribution of

stresses at the notch section, resulting in the concentration at the root. The fact that a corresponding strain concentration was not apparent in the moiré fringe analysis of this type of specimen may be due to inherent lack of sensitivity of the moiré technique near specimen boundaries, and also to the likelihood that the machined vee-notch was less than perfect, having a small but finite radius that substantially reduced the stress concentration. The modified Iosipescu (fillet notch) specimen did not exhibit a notch root stress concentration according to the finite element analysis and did possess a wide region, about three fourths of the net specimen depth, in which the shear stress was uniform. The analytical results point to this specimen configuration as probably the most satisfactory for all aspects of shear testing of composite materials. More comprehensive analytical studies of this specimen geometry are needed to determine the most appropriate notch depth and radius to achieve a closer approximation to uniform pure shear and a higher probability of shear failure away from the notch root. The analytical studies to optimize geometry should be supplemented by additional tests on specimens of selected composite laminates and also by photoelastic studies on orthotropic models.

Another aspect of the AFPB test which was mentioned briefly in Section IV concerns the development of friction forces between the load fixture and the specimen. The most likely place for this to occur is at any of the various load points where relative motion impends or takes place as the shear specimen undergoes deformation. An equilibrium analysis of the specimen and test fixture shows that friction forces cannot affect the distribution of vertical forces to the specimen. The specimen shear stresses should then be unaffected by the presence of the friction forces; however, the latter will result in normal stresses parallel to the specimen axis. The consequence of this is to change the stress condition from pure shear to combined tension or compression and shear. Another effect of the friction forces would be to induce an apparent hysteresis effect in a load-unload test cycle which would obscure the actual stress-strain behavior of the test material. As noted previously, this was actually observed during tests on aluminum specimens. Axial strain measurements on aluminum specimens also indicated that these normal stresses are very small relative to the shear stresses and, consequently, should not have a noticeable effect on either the stress-strain behavior or failure conditions. However, the spurious hysteresis effect could be undesirable in certain test situations; therefore, some modification of the test fixture is warranted which would permit small, lateral specimen displacements at the various loading points.

Finally, some mention of other potential applications for the AFPB test method is worthwhile at this point. The test method is not limited by any means to in-plane shear measurements of composite materials. It is not, in fact, limited to use on composite materials, although there does not seem to be an essential requirement for a shear test on materials such as metals. In addition to the characterization of shear strength and stress-strain response, as presented in this report, the AFPB test method could be used to study other in-plane characteristics such as notch sensitivity or fracture toughness under pure shear loading. Moreover, it could be used to determine interlaminar shear properties of laminates and would also appear to be useful for measuring the shear strength and compliance of adhesive joints in any type of material. The AFPB test method does require further refinement; however, it has been demonstrated to be a satisfactory procedure by comparison with current test methods. It is recommended therefore that development of the AFPB method be continued along the lines suggested with the goal of producing a standardized test method for characterization of composite materials.

DISTRIBUTION LIST

No. of Copies	To
1	Office of the Director, Defense Research and Engineering, The Pentagon, Washington, D. C. 20301
	Metals and Ceramics Information Center, 505 King Avenue, Columbus, Ohio 43201
1	ATTN: Mr. Harold Mindlin, Director
1	Mr. James Lynch, Assistant Director
2	Mr. Daniel Maykuth
12	Commander, Defense Documentation Center, Cameron Station, Building 5, 5010 Duke Street, Alexandria, Virginia 22314
1	Advanced Research Projects Agency, The Pentagon, Washington, D. C. 20315
	Commander, U.S. Army Foreign Science and Technology Center, 220 Seventh Street, N.E., Charlottesville, Virginia 22901
1	ATTN: DRXST-SD3
	Office of the Deputy Chief of Staff for Research, Development, and Acquisition, Washington, D.C. 20310
1	ATTN: DAMA-ARZ-E
1	DAMA-CSS
	Commander, Army Research Office, P.O. Box 12211, Research Triangle Park, North Carolina 27709
1	ATTN: Dr. George Mayer
1	Mr. J. J. Murray
	Commander, U.S. Army Materiel Development and Readiness Command, 5001 Eisenhower Avenue, Alexandria, Virginia 22333
1	ATTN: DRCQA-E
1	DRCQA-P
1	DRCDE-D
1	DRCDMD-FT
1	DRCLDC
1	DRCMT
1	DRCMM-M
	Commander, U.S. Army Electronics Research and Development Command, Fort Monmouth, New Jersey 07703
2	ATTN: DRSEL-PA-E, Mr. Stan Alster
	Commander, U.S. Army Missile Research and Development Command, Redstone Arsenal, Alabama 35809
2	ATTN: DRDMI-TB, Redstone Scientific Information Center
1	DRDMI-TK, Mr. J. Alley
1	DRDMI-M
1	DRDMI-ET, Mr. Robert O. Black
1	DRDMI-QS, Mr. George L. Stewart, Jr.
1	DRDMI-EAT, Mr. R. Talley
1	DRDMI-QP
1	DRDMI-IE, Mr. J. E. Kirshtein
1	DRDMI-R, Mr. John L. McDaniel
1	Chief Scientist, Dr. W. W. Carter
1	Directorate of R&D
1	Dr. B. Steverding
	Commander, U.S. Army Troop Support and Aviation Materiel Readiness Command, 4300 Goodfellow Boulevard, St. Louis, Missouri 63120
1	ATTN: DRSTS-PLE, Mr. J. Corwin
1	DRSTS-Q
1	DRSTS-M
	Commander, U.S. Army Natick Research and Development Command, Natick, Massachusetts 01760
1	ATTN: DRDNA-EM
1	Technical Library
1	Dr. E. W. Ross
1	DRDNA-UE, Dr. L. A. McClaine
	Commander, U.S. Army Satellite Communications Agency, Fort Monmouth, New Jersey 07703
1	ATTN: Technical Document Center
	Commander, U.S. Army Tank-Automotive Research and Development Command, Warren, Michigan 48090
1	ATTN: DRDTA-RKA
2	DRDTA-UL, Technical Library
1	DRDTA-RKA, Mr. D. Matichuk
1	DRDTA-RKA, Mr. R. Dunec
1	DRDTA-RKA, Mr. S. Catalano
1	DRDTA-RH, Mr. O. Renius
1	DRDTA-JA, Mr. C. Kedzior
1	DRDTA-PPS, Mr. David Siegel
1	Mr. B. A. Schevo
	Commander, U.S. Army Tank-Automotive Materiel Readiness Command, Warren, Michigan 48090
2	ATTN: DRSTA-Q
	Commander, White Sands Missile Range, New Mexico 88002
1	ATTN: STEWS-WS-VT
1	STEWS-AD-L
1	STEWS-ID
1	STEWS-TD-PM

No. of Copies	To
	Commander, U.S. Army Mobility Equipment Research and Development Command, Fort Belvoir, Virginia 22060
1	ATTN: DRDME-D
1	DRDME-E
1	DRDME-G
1	DRDME-H
1	DRDME-M
1	DRDME-T
1	DRDME-TQ
1	DRDME-V
1	DRDME-ZE
1	DRDME-N
	Commander, U.S. Army Mobility Equipment Research and Development Command, 4300 Goodfellow Boulevard, St. Louis, Missouri 63120
1	ATTN: DRDME-PLC, Mr. J. Murphy
	Commander, U.S. Army Armament Materiel Readiness Command, Rock Island, Illinois 61201
2	ATTN: DRSAR-QA
1	DRSAR-SC
1	DRSAR-RDP
1	DRSAR-EN
1	DRSAR-QAE
	Commander, Rock Island Arsenal, Rock Island, Illinois 61299
1	ATTN: SARRI-EN, Mr. W. M. Kisner
1	SARRI-ENM, Mr. W. D. McHenry
1	SARRI-QA
	Commander, U.S. Army Armament Research and Development Command, Dover, New Jersey 07801
1	ATTN: DRDAR-LC, Mr. E. Kelly
1	DRDAR-LCA, Dr. Sharkoff
1	DRDAR-LCE, Dr. Walker
5	DRDAR-QAS, Mr. F. Fitzsimmons
1	DRDAR-SCM, Mr. J. D. Corrie
1	DRDAR-TSP, Mr. B. Stephans
2	DRDAR-TSS, (STINFO)
	Commander, Chemical Systems Laboratory, Aberdeen Proving Ground, Maryland 21010
1	ATTN: DRDAR-CLD, Mr. W. E. Montanary
	Commander, ARRADCOM, Product Assurance Directorate, Aberdeen Proving Ground, Maryland 21010
1	ATTN: DRDAR-QAC-E, Dr. W. J. Maurits
	Commander, Watervliet Arsenal, Watervliet, New York 12189
1	ATTN: DRDAR-LCB, Mr. T. Moraczewski
1	Dr. T. Davidson
1	Mr. D. P. Kendall
1	Mr. J. F. Throop
	Commander, U.S. Army Aviation Research and Development Command, St. Louis, Missouri 63166
1	ATTN: DRDAV-EXT
1	DRDAV-QR
1	DRDAV-QP
1	DRDAV-QE
1	DRDAV-LEP, Mr. J. M. Thorp
1	DRDAV-ER, Dr. I. Peterson
	Director, U.S. Army Industrial Base Engineering Activity, Rock Island, Illinois 61201
1	ATTN: DRXPE-MT, Mr. D. Brim
	Commander, Harry Diamond Laboratories, 2800 Powder Mill Road, Adelphi, Maryland 20783
1	ATTN: DRXDO-EDE, Mr. B. F. Willis
1	Technical Information Office
	Commander, U.S. Army Test and Evaluation Command, Aberdeen Proving Ground, Maryland 21005
1	ATTN: DRSTE-TD
1	DRSTE-ME
	Commander, U.S. Army Yuma Proving Ground, Yuma, Arizona 85364
1	ATTN: Technical Library
	Commander, Aberdeen Proving Ground, Maryland 21005
1	ATTN: STEAP-TL, Bldg. 305
1	STEAP-MT
1	STEAP-MT-M, Mr. J. A. Feroli
1	STEAP-MT-G, Mr. R. L. Huddleston
	Commander, U.S. Army Aeromedical Research Unit, P. O. Box 577, Fort Rucker, Alabama 36460
1	ATTN: Technical Library
	Commander, U.S. Army Tropic Test Center, Fort Clayton, Canal Zone
1	ATTN: STETC-TD, Drawer 942
	Commander, Picatinny Arsenal, Dover, New Jersey 07801
1	ATTN: Mr. A. Devine
1	Feltman Research Laboratories

No. of Copies	To
	Commander, U.S. Army Ballistic Research Laboratories, Aberdeen Proving Ground, Maryland 21005
1	ATTN: Dr. D. Eichelberger
1	Dr. R. Vitali
1	Dr. G. L. Filbey
1	Dr. W. Gillich
	Chief, Benet Weapons Laboratory, LCWSL, USA ARRADCOM, Watervliet Arsenal, Watervliet, New York 12189
1	ATTN: DRDAR-LCB-TL
	Director, Eustis Directorate, U.S. Army Air Mobility Research and Development Laboratory, Fort Eustis, Virginia 23604
1	ATTN: Mr. J. Robinson, DAVDL-E-MOS (AVRADCOM)
1	Mr. R. Berresford
	U.S. Army Aviation Training Library, Fort Rucker, Alabama 36360
1	ATTN: Buildings 5906-5907
	Commander, U.S. Army Agency for Aviation Safety, Fort Rucker, Alabama 36362
1	ATTN: Librarian, Building 4905
	Commander, USACDC Air Defense Agency, Fort Bliss, Texas 79916
1	ATTN: Technical Library
	Commander, U.S. Army Engineer School, Fort Belvoir, Virginia 22060
1	ATTN: Library
	Commander, U.S. Army Engineer Waterways Experiment Station, Vicksburg, Mississippi 39180
1	ATTN: Research Center Library
	Director, U.S. Army Materiel Systems Analysis Activity, Aberdeen Proving Ground, Maryland 21005
1	ATTN: AMXSY-D, Dr. J. Sperrazza
	Commander, U.S. Army Production Equipment Agency, Manufacturing Technology Branch, Rock Island Arsenal, Illinois 61202
1	ATTN: AMXPE, Mr. Ralph Siegel
	Commander, U.S. Army Research and Engineering Directorate, Warren, Michigan 48090
1	ATTN: SMOTA-RCM.1, Mr. Edward Moritz
1	SMOTA-RCM.1, Mr. Donald Phelps
	Commander, U.S. Army Cold Region Test Center, APO Seattle, Washington 98733
1	ATTN: STECR-OP-PM
	Commander, U.S. Army Dugway Proving Ground, Dugway, Utah 84022
1	ATTN: STEDP-MT
	Commander, U.S. Army Electronic Proving Ground, Fort Huachuca, Arizona 85613
1	ATTN: STEEP-MT
	Commander, Jefferson Proving Ground, Madison, Indiana 47250
1	ATTN: STEJP-TD-I
	Commander, U.S. Army Aircraft Development Test Activity, Fort Rucker, Alabama 36362
1	ATTN: STEBG-TD
	President, U.S. Army Armor and Engineer Board, Fort Knox, Kentucky 40121
1	ATTN: ATZKOAE-TA
	President, U.S. Army Field Artillery Board, Fort Sill, Oklahoma 73503
1	ATTN: ATZR-BDOP
	Commander, Anniston Army Depot, Anniston, Alabama 36202
1	ATTN: SDSAN-QA
	Commander, Corpus Christi Army Depot, Corpus Christi, Texas 78419
1	ATTN: SDSCC-MEE, Mr. Haggerty, Mail Stop 55
	Commander, Letterkenny Army Depot, Chambersburg, Pennsylvania 17201
1	ATTN: SDS-LE-QA
	Commander, Lexington-Bluegrass Army Depot, Lexington, Kentucky 40507
1	ATTN: SDSRR-QA
	Commander, New Cumberland Army Depot, New Cumberland, Pennsylvania 17070
1	ATTN: SDSNC-QA
	Commander, U.S. Army Depot Activity, Pueblo, Colorado 81001
2	ATTN: SDSTE-PU-Q
	Commander, Red River Army Depot, Texarkana, Texas 75501
1	ATTN: SDSRR-QA
	Commander, Sacramento Army Depot, Sacramento, California 95813
1	ATTN: SDSSA-QA
	Commander, Savanna Army Depot Activity, Savanna, Illinois 61074
1	ATTN: SDSSV-S

No. of Copies	To
	Commander, Seneca Army Depot, Romulus, New York 14541
1	ATTN: SDSSE-R
	Commander, Sharpe Army Depot, Lathrop, California 95330
1	ATTN: SDSSH-QE
	Commander, Sierra Army Depot, Herlong, California 96113
1	ATTN: SDSSI-DQA
	Commander, Tobyhanna Army Depot, Tobyhanna, Pennsylvania 18466
1	ATTN: SDSTO-Q
	Commander, Tooele Army Depot, Tooele, Utah 84074
1	ATTN: SDSTE-QA
	Director, DARCOM Ammunition Center, Savanna, Illinois 61074
1	ATTN: SARAC-DE
1	Chief, Bureau of Naval Weapons, Department of the Navy, Room 2225, Munitions Building, Washington, D. C.
	Chief, Bureau of Ships, Department of the Navy, Washington, D. C. 20315
1	ATTN: Code 341
	Chief of Naval Research, Arlington, Virginia 22217
1	ATTN: Code 471
	Commander, Naval Air Engineering Center, Lakehurst, New Jersey 08733
1	ATTN: Technical Library, Code 1115
	Director, Structural Mechanics Research, Office of Naval Research, 800 North Quincy St., Arlington, Virginia 22203
1	ATTN: Dr. N. Perrone
	Naval Air Development Center, Aero Materials Department, Warminster, Pennsylvania 18974
1	ATTN: J. Viglione
	David Taylor Naval Ship Research and Development Laboratory, Annapolis, Maryland 21402
1	ATTN: Dr. H. P. Chu
	Naval Underwater Systems Center, New London, Connecticut 06320
1	ATTN: R. Kasper
	Naval Research Laboratory, Washington, D. C. 20375
1	ATTN: C. D. Beachem, Head, Adv. Mat'ls Tech Br. (Code 6310)
1	Dr. J. M. Krafft - Code 8430
	Naval Weapons Laboratory, Washington, D. C. 20390
1	ATTN: H. W. Romine, Mail Stop 103
	Headquarters, U. S. Air Force/RDPI, The Pentagon, Washington, D. C. 20330
1	ATTN: Major Donald Sponberg
	Headquarters, Aeronautical Systems Division, 4950 TEST W/TZHP (DH 2-5 Mgr), Wright-Patterson Air Force Base, Ohio 45433
1	ATTN: AFML-MATB, Mr. George Glenn
2	AFML-MXE, E. Morrissey
1	AFML-LLP, D. M. Forney, Jr.
1	AFML-LC
1	AFML-MBC, S. Schulman
1	Dr. S. Tsai
1	Dr. N. Pagano
	Air Force Flight Dynamics Laboratory, Wright-Patterson Air Force Base, Ohio 45433
1	ATTN: AFFDL (FBS), C. Wallace
1	AFFDL (FBE), G. D. Sendeckyj
1	AFFDL (FB), Dr. J. C. Halpin
	National Aeronautics and Space Administration, Washington, D. C. 20546
1	ATTN: AFSS-AD, Office of Scientific & Technical Information
1	Mr. B. G. Achhammer
1	Mr. G. C. Deutsch - Code RW
	National Aeronautics and Space Administration, Marshall Space Flight Center, Huntsville, Alabama 35812
1	ATTN: R. J. Schwinghamer, EH01, Director M&P Laboratory
1	Mr. W. A. Wilson, EH41, Building 4612
	Albany Metallurgy Research Center, Albany, Oregon 97321
1	ATTN: Mr. R. R. Wells, Research Director
	Defense Materials Service, General Services Administration, Washington, D. C. 20405
1	ATTN: Mr. Clarence A. Fredell, Director, Technical R&D Staff
	National Aeronautics and Space Administration, Langley Research Center, Hampton, Virginia 23665
1	ATTN: Mr. H. F. Hardrath, Mail Stop 188M
1	Mr. R. Foye, Mail Stop 188A

No. of Copies	To
	Wyman-Gordon Company, Worcester, Massachusetts 01601
1	ATTN: Technical Library
	Lockheed-Georgia Company, 86 South Cobb Drive, Marietta, Georgia 30063
1	ATTN: Materials & Processes Eng. Dept. 71-11, Zone 54
	National Bureau of Standards, U. S. Department of Commerce, Washington, D. C. 20234
1	ATTN: Mr. J. A. Bennett
1	Mechanical Properties Data Center, Belfour Stulen Inc., 13917 W. Bay Shore Drive, Traverse City, Michigan 49684
1	Mr. W. F. Anderson, Atomics International, Canoga Park, California 91303
	Midwest Research Institute, 425 Coker Boulevard, Kansas City, Missouri 64110
1	ATTN: Mr. C. Q. Bowles
1	Dr. J. Charles Grosskreutz, Asst. Dir. for Research, Solar Energy Research Institute, 1536 Cole Boulevard, Golden, Colorado 80401
1	Mr. A. Hurlich, Convair Div., General Dynamics Corp., Mail Zone 630-01, P. O. Box 80847, San Diego, California 92138
	Virginia Polytechnic Institute and State University, Department of Engineering Mechanics, 230 Norris Hall, Blacksburg, Virginia 24061
1	ATTN: Prof. R. M. Barker
1	Assoc. Prof. G. W. Swift
	Southwest Research Institute, 8500 Culebra Road, San Antonio, Texas 78284
1	ATTN: Mr. G. C. Grimes
	IIT Research Institute, Chicago, Illinois 60616
1	ATTN: Dr. I. M. Daniel
1	Mr. J. G. Kaufman, Alcoa Research Laboratories, New Kensington, Pennsylvania 15068
1	Mr. G. M. Orner, MANLABS, 21 Erie Street, Cambridge, Massachusetts 02139
1	Mr. P. N. Randall, TRW Systems Group — O-1/2210, One Space Park, Redondo Beach, California 90278
1	Dr. E. A. Steigerwald, TRW Metals Division, P. O. Box 250, Minerva, Ohio 44657
1	Dr. George R. Irwin, Department of Mechanical Engineering, University of Maryland, College Park, Maryland 20742
1	Mr. W. A. Van der Sluys, Research Center, Babcock and Wilcox, Alliance, Ohio 44601
1	Mr. B. M. Wundt, 2346 Shirl Lane, Schenectady, New York 12309
	Battelle Columbus Laboratories, 505 King Avenue, Columbus, Ohio 43201
1	ATTN: Dr. E. Rybicki
1	Dr. K. R. Merckx, Battelle Northwest Institute, Richland, Washington 99352
	General Electric Company, Schenectady, New York 12010
1	ATTN: Mr. A. J. Brothers, Materials & Processes Laboratory
	General Electric Company, Knolls Atomic Power Laboratory, P. O. Box 1072, Schenectady, New York 12301
1	ATTN: Mr. F. J. Mehringer
1	Dr. L. F. Coffin, Room 1C41-K1, Corp. R&D, General Electric Company, P. O. Box 8, Schenectady, New York 12301
	United States Steel Corporation, Monroeville, Pennsylvania 15146
1	ATTN: Dr. A. K. Shoemaker, Research Laboratory, Mail Stop 78
	Westinghouse Electric Company, Bettis Atomic Power Laboratory, P. O. Box 109, West Mifflin, Pennsylvania 15122
1	ATTN: Mr. M. L. Parrish
	Westinghouse Research and Development Center, 1310 Beulah Road, Pittsburgh, Pennsylvania 15235
1	ATTN: Mr. E. T. Wessel
	Mr. J. Manjoine
1	Dr. Alan S. Tetelman, Failure Analysis Associates, Suite 4, 11777 Mississippi Ave., Los Angeles, California 90025

No. of Copies	To
	Brown University, Providence, Rhode Island 02912
1	ATTN: Prof. J. R. Rice
1	Prof. W. N. Findley, Division of Engineering, Box D
	Carnegie-Mellon University, Department of Mechanical Engineering, Schenley Park, Pittsburgh, Pennsylvania 15213
1	ATTN: Dr. J. L. Swedlow
1	Prof. J. Dvorak, Civil Engineering Department, Duke University, Durham, North Carolina 27706
	George Washington University, School of Engineering and Applied Sciences, Washington, D. C. 20052
1	ATTN: Dr. H. Liebowitz
	Lehigh University, Bethlehem, Pennsylvania 18015
1	ATTN: Prof. G. C. Sih
1	Prof. F. Erodgan
	Massachusetts Institute of Technology, Cambridge, Massachusetts 02139
1	ATTN: Prof. F. A. McClintock, Room 1-304
1	Prof. T. H. H. Pian, Department of Aeronautics and Astronautics
1	Prof. F. J. McGarry
1	Prof. A. S. Argon, Room 1-306
1	Prof. J. N. Rossettos, Department of Mechanical Engineering, Northeastern University, Boston, Massachusetts 02115
1	Prof. R. Greif, Department of Mechanical Engineering, Tufts University, Medford, Massachusetts 02155
1	Dr. D. E. Johnson, AVCO Systems Division, Wilmington, Massachusetts 01887
	University of Delaware, Department of Aerospace and Mechanical Engineering, Newark, Delaware 19711
1	ATTN: Prof. B. Pipes
1	Prof. J. Vinson
1	Prof. W. Goldsmith, Department of Mechanical Engineering, University of California, Berkeley, California 94720
	University of California, Los Alamos Scientific Laboratory, Los Alamos, New Mexico 87544
1	ATTN: Dr. R. Karpp
1	Prof. A. J. McEvily, Metallurgy Department U-136, University of Connecticut, Storrs, Connecticut 06268
1	Prof. D. Drucker, Dean of School of Engineering, University of Illinois, Champaign, Illinois 61820
	University of Illinois, Urbana, Illinois 61801
1	ATTN: Prof. H. T. Corten, Department of Theoretical and Applied Mechanics, 212 Talbot Laboratory
1	Dr. M. L. Williams, Dean of Engineering, 240 Benedum Hall, University of Pittsburgh, Pittsburgh, Pennsylvania 15260
1	Prof. A. Kobayashi, Department of Mechanical Engineering, FU-10, University of Washington, Seattle, Washington 98195
1	Mr. W. A. Wood, Baillieu Laboratory, University of Melbourne, Melbourne, Australia
1	Mr. Elmer Wheeler, Airesearch Manufacturing Company, 402 S. 36th Street, Phoenix, Arizona 85034
1	Mr. Charles D. Roach, U.S. Army Scientific and Technical Information Team, 6000 Frankfurt/Main, I. G. Hochhaus, Room 750, West Germany (APO 09710, NY)
1	Prof. R. Jones, Department of Civil Engineering, Ohio State University, 206 W. 18th Avenue, Columbus, Ohio 43210
	State University of New York at Stony Brook, Stony Brook, New York 11790
1	ATTN: Prof. Fu-Pen Chiang, Department of Mechanics
	E. I. Du Pont de Nemours and Company, Wilmington, Delaware 19898
1	ATTN: Dr. Carl Zweben, Industrial Fibers Division, Textile Fibers Department
	Lawrence Livermore Laboratory, Livermore, California 94550
1	ATTN: Dr. E. M. Wu
	Director, Army Materials and Mechanics Research Center, Watertown, Massachusetts 02172
2	ATTN: DRXMR-PL
1	DRXMR-AG-MD
3	Authors

Army Materials and Mechanics Research Center,
Watertown, Massachusetts 02172
IN-PLANE SHEAR TEST FOR COMPOSITE MATERIALS –
John M. Slepetz, Theodore F. Zagaeski, and
Robert F. Novello

Technical Report AMMRC TR 78-30, July 1978, 22 pp –
illus-tables, D/A Project M726350, MTT Project

AD ____________

UNCLASSIFIED
UNLIMITED DISTRIBUTION

Key Words

Fiber-reinforced composites
Shear properties
Shear strength

A new method for characterizing the in-plane shear properties of composite materials is discussed. The method employs an asymmetrical four-point bending (AFPB) load arrangement which subjects the test specimen to pure shear at its centerline: the shear stress distribution at this location is uniform or otherwise depending upon the specimen geometry. Demonstration tests were conducted on specimens of aluminum and two types of fiber-reinforced composites of various specimen geometries including rectangular, vee-notched rectangular, and fillet-notched rectangular. In addition, a finite element analysis of these specimen configurations was undertaken to determine the depthwise stress distribution in each case. Strain measurements on test specimens showed a parabolic distribution in rectangular specimens and a uniform distribution in vee-notched specimens. The finite element analysis, however, showed a stress concentration at the notch root in the latter case, and specimens loaded to destruction tended to fail at the notch. It was concluded that with appropriate modification in the test fixture and specimen geometry the AFPB method developed will be an effective test procedure for measurement of in-plane shear properties.

Army Materials and Mechanics Research Center,
Watertown, Massachusetts 02172
IN-PLANE SHEAR TEST FOR COMPOSITE MATERIALS –
John M. Slepetz, Theodore F. Zagaeski, and
Robert F. Novello

Technical Report AMMRC TR 78-30, July 1978, 22 pp –
illus-tables, D/A Project M726350, MTT Project

AD ____________

UNCLASSIFIED
UNLIMITED DISTRIBUTION

Key Words

Fiber-reinforced composites
Shear properties
Shear strength

A new method for characterizing the in-plane shear properties of composite materials is discussed. The method employs an asymmetrical four-point bending (AFPB) load arrangement which subjects the test specimen to pure shear at its centerline: the shear stress distribution at this location is uniform or otherwise depending upon the specimen geometry. Demonstration tests were conducted on specimens of aluminum and two types of fiber-reinforced composites of various specimen geometries including rectangular, vee-notched rectangular, and fillet-notched rectangular. In addition, a finite element analysis of these specimen configurations was undertaken to determine the depthwise stress distribution in each case. Strain measurements on test specimens showed a parabolic distribution in rectangular specimens and a uniform distribution in vee-notched specimens. The finite element analysis, however, showed a stress concentration at the notch root in the latter case, and specimens loaded to destruction tended to fail at the notch. It was concluded that with appropriate modification in the test fixture and specimen geometry the AFPB method developed will be an effective test procedure for measurement of in-plane shear properties.

Army Materials and Mechanics Research Center,
Watertown, Massachusetts 02172
IN-PLANE SHEAR TEST FOR COMPOSITE MATERIALS –
John M. Slepetz, Theodore F. Zagaeski, and
Robert F. Novello

Technical Report AMMRC TR 78-30, July 1978, 22 pp –
illus-tables, D/A Project M726350, MTT Project

AD ____________

UNCLASSIFIED
UNLIMITED DISTRIBUTION

Key Words

Fiber-reinforced composites
Shear properties
Shear strength

A new method for characterizing the in-plane shear properties of composite materials is discussed. The method employs an asymmetrical four-point bending (AFPB) load arrangement which subjects the test specimen to pure shear at its centerline: the shear stress distribution at this location is uniform or otherwise depending upon the specimen geometry. Demonstration tests were conducted on specimens of aluminum and two types of fiber-reinforced composites of various specimen geometries including rectangular, vee-notched rectangular, and fillet-notched rectangular. In addition, a finite element analysis of these specimen configurations was undertaken to determine the depthwise stress distribution in each case. Strain measurements on test specimens showed a parabolic distribution in rectangular specimens and a uniform distribution in vee-notched specimens. The finite element analysis, however, showed a stress concentration at the notch root in the latter case, and specimens loaded to destruction tended to fail at the notch. It was concluded that with appropriate modification in the test fixture and specimen geometry the AFPB method developed will be an effective test procedure for measurement of in-plane shear properties.

Army Materials and Mechanics Research Center,
Watertown, Massachusetts 02172
IN-PLANE SHEAR TEST FOR COMPOSITE MATERIALS –
John M. Slepetz, Theodore F. Zagaeski, and
Robert F. Novello

Technical Report AMMRC TR 78-30, July 1978, 22 pp –
illus-tables, D/A Project M726350, MTT Project

AD ____________

UNCLASSIFIED
UNLIMITED DISTRIBUTION

Key Words

Fiber-reinforced composites
Shear properties
Shear strength

A new method for characterizing the in-plane shear properties of composite materials is discussed. The method employs an asymmetrical four-point bending (AFPB) load arrangement which subjects the test specimen to pure shear at its centerline: the shear stress distribution at this location is uniform or otherwise depending upon the specimen geometry. Demonstration tests were conducted on specimens of aluminum and two types of fiber-reinforced composites of various specimen geometries including rectangular, vee-notched rectangular, and fillet-notched rectangular. In addition, a finite element analysis of these specimen configurations was undertaken to determine the depthwise stress distribution in each case. Strain measurements on test specimens showed a parabolic distribution in rectangular specimens and a uniform distribution in vee-notched specimens. The finite element analysis, however, showed a stress concentration at the notch root in the latter case, and specimens loaded to destruction tended to fail at the notch. It was concluded that with appropriate modification in the test fixture and specimen geometry the AFPB method developed will be an effective test procedure for measurement of in-plane shear properties.

Army Materials and Mechanics Research Center,
Watertown, Massachusetts 02172
IN-PLANE SHEAR TEST FOR COMPOSITE MATERIALS –
John M. Slepetz, Theodore F. Zagaeski, and
Robert F. Novello

Technical Report AMMRC TR 78-30, July 1978, 22 pp –
illus-tables, D/A Project M726350, MTT Project

AD ______________

UNCLASSIFIED
UNLIMITED DISTRIBUTION

Key Words

Fiber-reinforced composites
Shear properties
Shear strength

A new method for characterizing the in-plane shear properties of composite materials is discussed. The method employs an asymmetrical four-point bending (AFPB) load arrangement which subjects the test specimen to pure shear at its centerline: the shear stress distribution at this location is uniform or otherwise depending upon the specimen geometry. Demonstration tests were conducted on specimens of aluminum and two types of fiber-reinforced composites of various specimen geometries including rectangular, vee-notched rectangular, and fillet-notched rectangular. In addition, a finite element analysis of these specimen configurations was undertaken to determine the depthwise stress distribution in each case. Strain measurements on test specimens showed a parabolic distribution in rectangular specimens and a uniform distribution in vee-notched specimens. The finite element analysis, however, showed a stress concentration at the notch root in the latter case, and specimens loaded to destruction tended to fail at the notch. It was concluded that with appropriate modification in the test fixture and specimen geometry the AFPB method developed will be an effective test procedure for measurement of in-plane shear properties.

Army Materials and Mechanics Research Center,
Watertown, Massachusetts 02172
IN-PLANE SHEAR TEST FOR COMPOSITE MATERIALS –
John M. Slepetz, Theodore F. Zagaeski, and
Robert F. Novello

Technical Report AMMRC TR 78-30, July 1978, 22 pp –
illus-tables, D/A Project M726350, MTT Project

AD ______________

UNCLASSIFIED
UNLIMITED DISTRIBUTION

Key Words

Fiber-reinforced composites
Shear properties
Shear strength

A new method for characterizing the in-plane shear properties of composite materials is discussed. The method employs an asymmetrical four-point bending (AFPB) load arrangement which subjects the test specimen to pure shear at its centerline: the shear stress distribution at this location is uniform or otherwise depending upon the specimen geometry. Demonstration tests were conducted on specimens of aluminum and two types of fiber-reinforced composites of various specimen geometries including rectangular, vee-notched rectangular, and fillet-notched rectangular. In addition, a finite element analysis of these specimen configurations was undertaken to determine the depthwise stress distribution in each case. Strain measurements on test specimens showed a parabolic distribution in rectangular specimens and a uniform distribution in vee-notched specimens. The finite element analysis, however, showed a stress concentration at the notch root in the latter case, and specimens loaded to destruction tended to fail at the notch. It was concluded that with appropriate modification in the test fixture and specimen geometry the AFPB method developed will be an effective test procedure for measurement of in-plane shear properties.

Army Materials and Mechanics Research Center,
Watertown, Massachusetts 02172
IN-PLANE SHEAR TEST FOR COMPOSITE MATERIALS –
John M. Slepetz, Theodore F. Zagaeski, and
Robert F. Novello

Technical Report AMMRC TR 78-30, July 1978, 22 pp –
illus-tables, D/A Project M726350, MTT Project

AD ______________

UNCLASSIFIED
UNLIMITED DISTRIBUTION

Key Words

Fiber-reinforced composites
Shear properties
Shear strength

A new method for characterizing the in-plane shear properties of composite materials is discussed. The method employs an asymmetrical four-point bending (AFPB) load arrangement which subjects the test specimen to pure shear at its centerline: the shear stress distribution at this location is uniform or otherwise depending upon the specimen geometry. Demonstration tests were conducted on specimens of aluminum and two types of fiber-reinforced composites of various specimen geometries including rectangular, vee-notched rectangular, and fillet-notched rectangular. In addition, a finite element analysis of these specimen configurations was undertaken to determine the depthwise stress distribution in each case. Strain measurements on test specimens showed a parabolic distribution in rectangular specimens and a uniform distribution in vee-notched specimens. The finite element analysis, however, showed a stress concentration at the notch root in the latter case, and specimens loaded to destruction tended to fail at the notch. It was concluded that with appropriate modification in the test fixture and specimen geometry the AFPB method developed will be an effective test procedure for measurement of in-plane shear properties.

Army Materials and Mechanics Research Center,
Watertown, Massachusetts 02172
IN-PLANE SHEAR TEST FOR COMPOSITE MATERIALS –
John M. Slepetz, Theodore F. Zagaeski, and
Robert F. Novello

Technical Report AMMRC TR 78-30, July 1978, 22 pp –
illus-tables, D/A Project M726350, MTT Project

AD ______________

UNCLASSIFIED
UNLIMITED DISTRIBUTION

Key Words

Fiber-reinforced composites
Shear properties
Shear strength

A new method for characterizing the in-plane shear properties of composite materials is discussed. The method employs an asymmetrical four-point bending (AFPB) load arrangement which subjects the test specimen to pure shear at its centerline: the shear stress distribution at this location is uniform or otherwise depending upon the specimen geometry. Demonstration tests were conducted on specimens of aluminum and two types of fiber-reinforced composites of various specimen geometries including rectangular, vee-notched rectangular, and fillet-notched rectangular. In addition, a finite element analysis of these specimen configurations was undertaken to determine the depthwise stress distribution in each case. Strain measurements on test specimens showed a parabolic distribution in rectangular specimens and a uniform distribution in vee-notched specimens. The finite element analysis, however, showed a stress concentration at the notch root in the latter case, and specimens loaded to destruction tended to fail at the notch. It was concluded that with appropriate modification in the test fixture and specimen geometry the AFPB method developed will be an effective test procedure for measurement of in-plane shear properties.

DEPARTMENT OF THE ARMY
ARMY MATERIALS AND MECHANICS RESEARCH CENTER
Watertown, Massachusetts 02172

OFFICIAL BUSINESS

POSTAGE AND FEES PAID
DEPARTMENT OF THE ARMY
DOD 314

THIRD CLASS MAIL